On-chip optical detection of laser cooled atoms

P. A. Quinto-Su, M. Tscherneck, M. Holmes and N. P. Bigelow

Department of Physics and Astronomy and The Laboratory for Laser Energetics
University of Rochester, Rochester, NY 14627

Abstract: We have used an optical fiber based system to implement optical detection of atoms trapped on a reflective "atom-chip". A fiber pair forms an emitter-detector setup that is bonded to the atom-chip surface to optically detect and probe laser cooled atoms trapped in a surface magneto-optical trap. We demonstrate the utility of this scheme by measuring the linewidth of the Cs D2 line at different laser intensities.

OCIS codes: (020.7010) Trapping; (040.1880) Detection; (060.2370) Fiber optics sensors; (140.3320) Laser cooling; (140.7010) Trapping; (300.1030) Absorption; (300.6210) Spectroscopy, atomic

References and links

1. W. Hansel, P. Hommelhoff, T.W. Hansch, J. Reichel, "Bose-Einstein condensation on a microelectronic chip," Nature **413**, 498-501 (2001).
2. D. Cassettari, B. Hessmo, R. Folman, T. Maier, and J. Schmiedmayer, "Beam Splitter for Guided Atoms," Phys. Rev. Lett **85**, 5483-5487 (2000).
3. D. Casserati, A. Chenet, R. Folman, A. Haase, B. Hessmo, P. Kruger, T. Maier, S. Schneider, T. Calarco, J. Schmiedmayer, "Micromanipulation of neutral atoms with nanofabricated structures," Appl. Phys. B **70**, 721-730 (2000).
4. J. Reichel, W. Hansel, P. Hommelhoff, T.W. Hansch, "Applications of integrated magnetic microtraps," Appl. Phys. B **72**, 81-89 (2001).
5. H. Ott, J. Fortagh, G. Schlotterbeck, A. Grossmann, and C. Zimmermann, "Bose-Einstein Condensation in a Surface Microtrap," Phys. Rev. Lett. **87**, 230401 (2001).
6. A.H. Barnett, S.P. Smith, M. Olshanii, K.S. Johnson, A.W. Adams, and M. Prentiss, "Substrate-based atom waveguide using guided two color evanescent light fields," PRA **61**, 023608 (2000).
7. P. Horak, B.G. Klappauf, A. Haase, R. Folman, J Schmiedmayer, P. Domokos, and E.A. Hinds, "Possibility of single-atom detection on a chip," PRA **67**, 043806 (2003).
8. A. Constable, Jinha Kim, J.Mervis, F. Zarinetchi, and M. Prentiss, "Demonstration of a fiber-optical light-force trap," Opt. Lett. **18**, 1867-1869 (1993).
9. E.R. Lyons and G.J. Sonek, "Confinement and bistability in a tapered hemispherically lensed optical fiber trap," Appl. Phys. Lett. **66**, 1584-1586, (1995).
10. R.C.Gauthier and A.Frangioudakis, "Optical Levitation Particle Delivery System for a Dual Bem Fiber Optic Trap," Appl. Opt. **39**, 26-33, (2000).
11. M.T. Renn, D. Montgomery, O. Vdovin, D.Z. Anderson, C.E. Wieman, and E.A. Cornell, "Laser-Guided Atoms in Hollow-Core Optical Fibers," Phys. Rev. Lett. **75**, 3253-3256, (1995).
12. The lensed fiber was obtained from the Corning division of photonic materials, corning optifocus.
13. E.R.I. Abraham and E.A. Cornell, "Teflon Feedthrough for Coupling Optical Fibers into Ultrahigh Vacuum Systems," Appl. Opt. **37**, 1762-1763 (1998).
14. M. Holmes, M. Tscherneck, P. A. Quinto-Su and N. P. Bigelow, "Isotopic difference in the heteronuclear loss rate in a two species surface trap," Phys. Rev. A **69**, 063408, (2004).
15. H.J. Metcalf, *Laser Cooling and Trapping*, (Springer, New York, 1999).
16. D.A. Steck, *Cesium D line Data.*
17. S. Kadlecek, J. Sebby, R. Newell, and T. G. Walker, "Nondestructive spatial heterodyne imaging of cold atoms," Opt. Lett. **26**, 137-139 (2001).
18. P.J. Fox, T.R. Mackin, L.D. Turner, I. Colton, K.A. Nugent, and R.E. Scholten, "Noninterferometric phase imaging of a neutral atomic beam," J. Opt. Soc. Am B **19**, 1773-1776 (2002).

#5189 - $15.00 US Received 2 September 2004; revised 1 October 2004; accepted 4 October 2004

19. R. Dumke, M. Volk, T. Muther, F.B.J. Buchkremer, G. Birkl, and W. Ertmer, "Micro-optical Realization of Arrays of Selectively Addressable Dipole Traps: A Scalable Configuration for Quantum Computation with Atomic Qubits," Phys. Rev. Lett. **89**, 097903 (2002).

1. Introduction

In the last few years there has been considerable progress on the manipulation and control of atomic motion using microfabricated wires bonded onto the surface of a silicon chip - the so called "atom chip". Atom traps, waveguides, beam splitters and even atomic BECs have been demonstrated using this exciting technology.[1–5] To date, this experimental work has focused on the use of on-chip current carrying structures, and hence magnetic interactions, to manipulate the atoms. More recently, there have been some proposals to integrate light sources onto the chip surface[6] and there has even been a recent proposal for using an optical waveguide based resonator attached to a chip surface to achieve high-efficiency single atom detection.[7] Although the use of waveguides and specifically fiber optics to manipulate small particles is well known,[8–10] comparatively little work has been reported which combines fiber optics with ultracold atoms, the exception being elegant work on atomic guiding in hollow core fibers.[11] So far, these two technologies - fiber optics and surface traps - have not been combined. Moreover, there has been little experimental progress using on-chip optical techniques to probe and manipulate atoms.

2. Experiment and results

In this paper, we present new results that combine the integration of surface atom control with "on-chip" optics. We demonstrate that fiber based optics can easily be combined with atom-chip structures by introducing a fiber optical waveguide onto a microfabricated atom chip device. In our experiments, two solid core optical fibers are chemically bonded onto the chip surface in a co-axial geometry. In this way, the light exiting one fiber is incident on the input aperture of the second fiber. As atoms pass through the gap between the fibers, the light interacts with the atoms and is scattered, decreasing the fiber-to-fiber coupling. In this way, on-chip probing and detection of atoms is realized. To demonstrate the utility of this system, we perform a simple spectroscopic measurement.

In our experiments, the fiber-to-fiber spacing is 4.5mm (see Fig. 1). Under normal circumstances, the rapidly diverging light exiting one of the fibers (the "source" fiber) would only weakly couple into the second "detection" fiber ($<$ 1% coupling efficiency), with a large portion of the light being scattered from the chip surface. To address this problem, to increase the coupling between the fibers, and to reduce spurious scattering, one of the two fibers in our experiments has an integrated spherical lens (f=2.5mm) on its output facet[12] that focuses the exiting light (beam waist $w_0 = 31\mu$m) onto the input facet of the "detection" fiber (Fig. 1). To achieve good coupling between the fibers, we also used a multimode fiber cleaved with a flat facet and a core diameter of 200μm as the detection fiber.

The probe light was coupled into the source fiber and the fiber was then passed into a high vacuum chamber ($p \leq 10^{-8}$Torr) and onto the atom chip. Part of the output power P_0 from this fiber was coupled into the second fiber which carried the light back out of the chamber. After exiting the fiber, the light was detected by a silicon photo diode (PD). To pass the fibers into and out of the vacuum chamber we followed the method demonstrated by Abraham *et. al*.[13] in which a flange with a Swagelock feedthrough is combined with a custom-made teflon ferrule penetrated by two holes to allow for the passage of the fibers.

The fiber setup is schematically shown in Fig. 2. The probe laser is an extended cavity diode laser (linewidth $<$ 1 MHz) stabilized with respect to a saturated absorption spectroscopy setup. The probe beam was switched using an acousto-optical modulator (AOM) at a frequency of

#5189 - $15.00 US Received 2 September 2004; revised 1 October 2004; accepted 4 October 2004

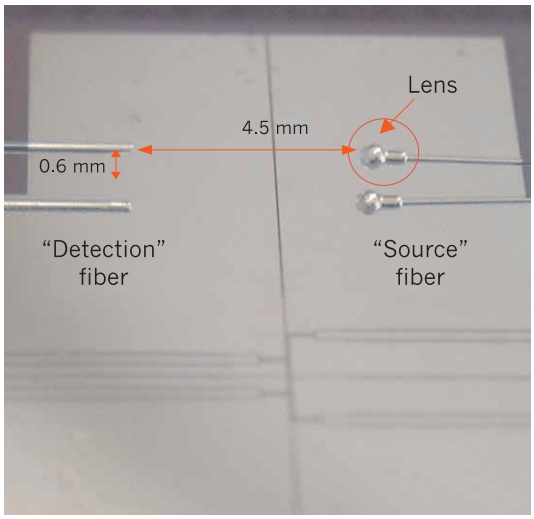

Fig. 1. Configuration of the optical fibers. The lensed fiber (right) is coupled to the laser and the multimode fiber (left) takes the light into a photo-detector. The “fibers” on the bottom are reflections from the mirrored surface. The dark lines on the surface are the contours of etched wires. The separation between the fibers and the height are 4.5 mm and 0.6 mm respectively.

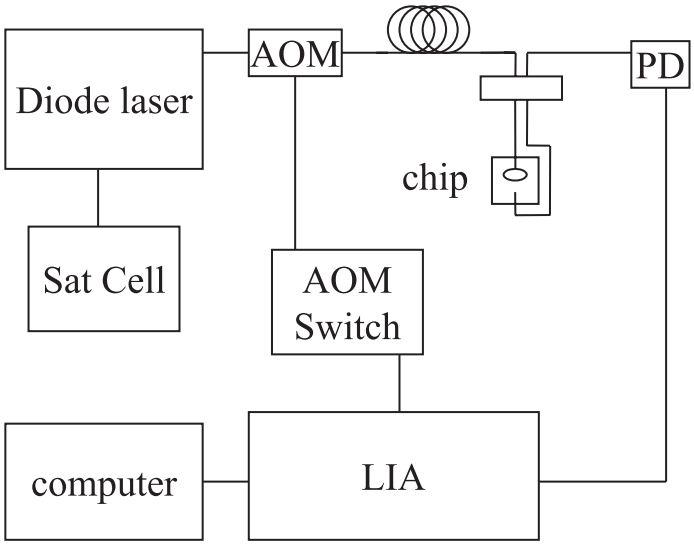

Fig. 2. Fiber experimental setup.

#5189 - $15.00 US
Received 2 September 2004; revised 1 October 2004; accepted 4 October 2004

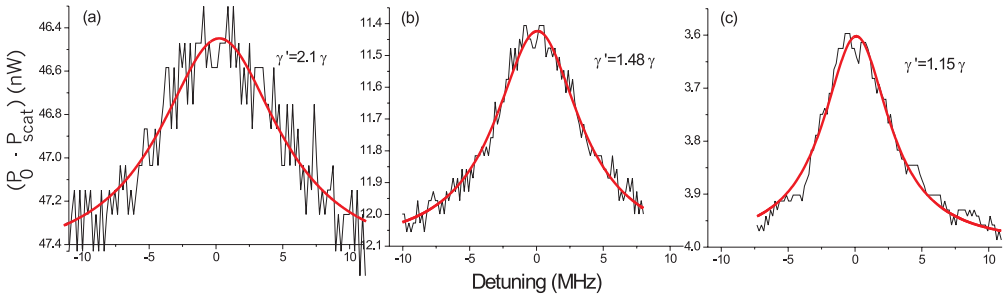

Fig. 3. Frequency scans for different intensities of the detection laser, the height of the peaks is the power scattered by the atoms. (a) I = 3.16 mW/cm^2, P_0 =55.4 nW with 1.4% scattered by the atoms. In (b) I = 0.8 mW/cm^2, P_0=12.1nW with 5% scattered. (c) I = 0.26 mW/cm^2, P_0=4 nW with 9.8% scattered.

70Hz. In addition to provide amplitude modulation, the AOM allowed fine frequency tuning of the probe laser. The output from the detection fiber was measured by the photo detector (PD) and processed using a lock-in-amplifier (LIA) synchronized to the AOM amplitude modulation. The power P_0 was adjusted using a half-wave plate and a polarizing beam-splitter cube. In the absence of atomic scatterers in the gap between the fibers, the power output onto the detector $P_{detected}$ can be written as TP_0, where T ($0 \leq T \leq 1$) is a transmission coefficient. T depends primarily on the characteristics of the individual fibers and on the geometry of the fiber system (e.g. on the separation d between the fibers). For our geometry the measured value of T is 0.37. A primary limitation of the coupling efficiency arises from parasitic reflections at the input facet of the detection fiber. Here we neglect the small ($\ll$0.1%) transmission losses in the fibers. When atoms are present in between the fibers, $P_{detected} \approx T(P_0\text{-}\alpha P_{scat})$, where P_{scat} is the power scattered out of the source beam by the atoms in the interaction zone between the fibers. α is a geometrical factor reflecting the fraction of the solid angle subtended by the detection fiber aperture available for recapturing scattered photons. In our geometry $\alpha \sim 1$. The atomic sample used for the experiments was provided by a cesium (Cs) mirror magneto-optical trap (MMOT), created at the atom-chip surface.[14] The trap was operated on the $6S_{1/2}$(F=4) $\rightarrow$ $6P_{3/2}$(F'=5) transition with a detuning of $\Delta \sim -\gamma = -2\pi \times 5.22$MHz. The repumping laser was tuned to the $6S_{1/2}$(F=3) $\rightarrow$ $6P_{1/2}$(F'=4) transition of the D1 line. Both trapping and repumping light were coupled through a single, single-mode optical fiber that served to spatially filter the trap light. The output of this fiber was then split into the needed trapping beams and relayed to the chamber. The result was a stable, compact atomic cloud with a diameter $\sim 500\mu$m containing $\sim 10^5$ atoms centered at the focus of the fiber emitter-detector pair. The center of the cloud was located using a CCD camera and was measured to be $\sim$0.6 mm above the chip surface.

After loading the trap, the probe laser was scanned over a $\pm$11MHz wide range centered around the $6S_{1/2}$(F=4) $\rightarrow$ $6P_{3/2}$(F'=5) atomic transition. Figure 3 shows typical absorption profiles obtained for different on-axis average intensities (defined as $2P_0/(\pi w_0^2)$) of the probe laser. We note that the vertical scale is inverted, so that we find peaks (instead of dips) for nearly resonant light. In (a) the on-axis intensity is 3.16 mW/cm^2, while in (b) I=0.8 mW/cm^2 and in (c) I=0.26 mW/cm^2. A Lorenzian lineshape was fitted to the data and the linewidth was extracted. The power level provided by the source fiber was then varied and the intensity dependent linewidth examined. Figure 4 shows the measured linewidth versus the on-axis intensity. To analyze the results, the variations in the observed linewidth can be understood as due to power broadening. A simplified expression for the power broadened linewidth is given

#5189 - $15.00 US Received 2 September 2004; revised 1 October 2004; accepted 4 October 2004

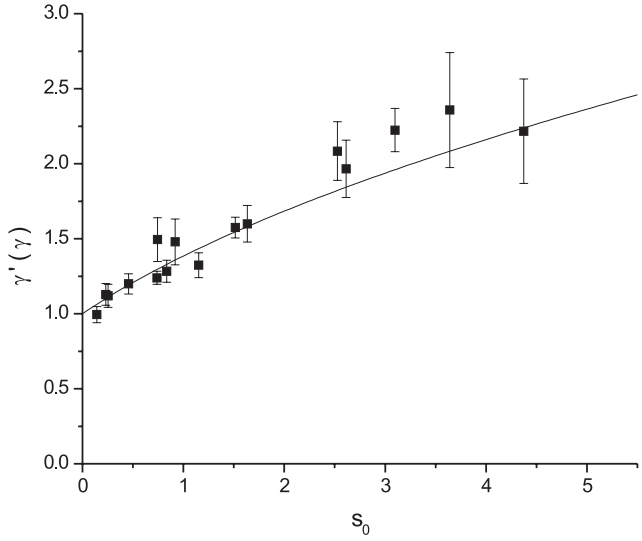

Fig. 4. Linewith as a function of $s_0 = I/I_s$. The line is the theoretical linewidth $\gamma = \gamma\sqrt{1+s_0}$

by $\gamma' = \gamma\sqrt{1+I/I_s}$, where I_s is the transition saturation intensity averaged over the relevant magnetic sub-levels.[15] The solid line is a plot of $\gamma'/2\pi$. The accepted value of the atomic natural linewidth of the Cs D2 line is $\gamma/2\pi = 5.22$MHz.[16] By fitting the function $\sqrt{1+I/I_s}$ to the data in Fig. 4 we obtain a meassurement of the natural linewidth $\gamma/2\pi$ as 5.35±0.5MHz, in good agreement with the accepted value.

In Fig. 5 we show the power absorbed by the atoms (height of the peaks) as a function of the probe power. We see the expected saturation of the scattered power as the probe power increases. We note that at higher powers, the on-resonance signal-to-noise ratio for atomic detection diminishes because the fraction of the power scattered by the atoms decreases: $P_{scatt} << P_0$. The net effect is that $P_0 - P_{scat} \sim P_0$ is small and approaches the detection noise level. Similarly, for powers below 5nW, the signal-to-noise ratio also decreases as we reach the detection noise floor of the photodiode. In the best case the signal to noise ratio was about 6. Using the data in Fig. 5 we find that the interaction volume contains approximately 600 atoms. With a signal-to-noise ratio of about 6, we can therefore place the on-resonance detection limit of our current set-up at approximately 100 atoms.

At the lowest powers ($\sim$ 2nW) measured scattering rates are as low as 0.18MHz. For these powers, the MMOT is hardly perturbed. An effect of the probe laser on the MMOT could only be seen for the highest laser powers.

3. Summary and conclusion

In summary, we have demonstrated a simple method for realizing an on-atom-chip optical system and have used this system to probe laser cooled atoms trapped at the surface. Significant improvements can be expected by using a lower noise photodetector and by applying anti-reflection coating to the input facet of the detection fiber. We are currently exploring these improvements, as well as off-resonant dispersive measurements ("non-destructive") in which the atom fiber pair is included in one arm of an optical interferometer. Related imaging methods

#5189 - $15.00 US Received 2 September 2004; revised 1 October 2004; accepted 4 October 2004

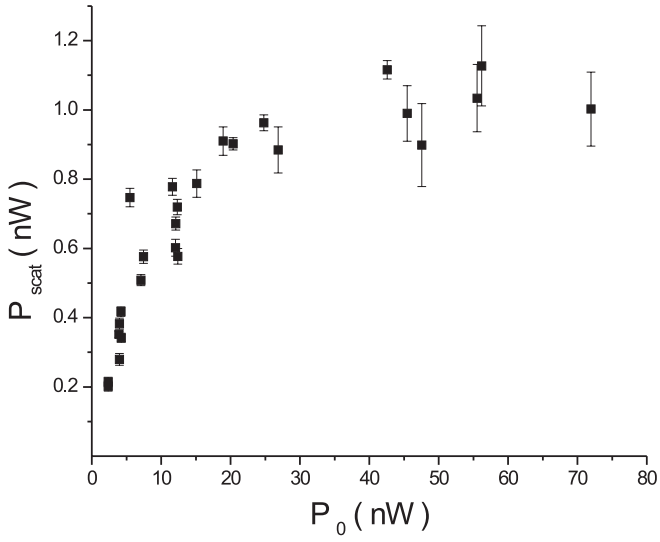

Fig. 5. Power absorbed by the MMOT as a function of probe power. The error bars are statistical errors from different runs.

have been demonstrated[17,18] with atomic beams and laser cooled atoms. Trapping of atoms at the focus of the fiber is also being explored using higher laser powers and large, red detunings.[19]

After the completion of this work we became aware of work done by Wang *et al*. implementing a Michelson interferometer on a chip.

Acknowledgments

This work was supported by the National Science Foundation, the Army Research Office and the University of Rochester.

#5189 - $15.00 US Received 2 September 2004; revised 1 October 2004; accepted 4 October 2004